LA-UR- 00-5437

Approved for public release; distribution is unlimited.

Title: CEM2K - Recent Developments in CEM

Author(s): Stepan G. Mashnik, Arnold J. Sierk, T-16
Theoretical Divison

Submitted to: Proceedings for The 2000 ANS/ENS International Meeting
Washington, DC, November 1-16, 2000

CEM2K - RECENT DEVELOPMENTS IN CEM

Stepan G. Mashnik and Arnold J. Sierk
Theoretical Division, Los Alamos National Laboratory, Los Alamos, NM 87545, USA

November 6, 2000

ABSTRACT

Recent developments of the Cascade-Exciton Model (CEM) of nuclear reactions are briefly described. These changes are motivated by new data on isotope production measured recently in "reverse kinematics" at GSI for interactions of ^{208}Pb and ^{238}U at 1 GeV/nucleon and ^{197}Au at 800 MeV/nucleon with liquid ^{1}H. This study leads us to CEM2k, which is a new version of the CEM code that is still under development. The increased accuracy and predictive power of the code CEM2k are shown by several examples. Further necessary work is outlined.

INTRODUCTION

The design of a hybrid reactor system driven with a high current accelerator requires information about residual nuclides that are produced by high energy protons interacting in the target and in structural materials. It is both physically and economically impossible to measure all necessary data, which is why reliable models and codes are needed. A model with a good predictive power both for the spectra of emitted particles and residual nuclide yields is the Cascade-Exciton Model (CEM) of nuclear reactions [1]. An improved version of the CEM is contained in the code CEM95 [2], which is available free from the NEA/OECD, Paris. Following an increased interest in intermediate-energy nuclear data in relation to such projects as Accelerator Transmutation of Wastes (ATW), Accelerator Production of Tritium (APT), and others, we developed a new version of the cascade-exciton model, CEM97 [3,4]. CEM97 has a number of improved physics features, uses better elementary-particle cross sections for the cascade model, and due to some significant algorithmic improvements is several times faster than CEM95. It has been incorporated into the recent transport code system MCNPX [5].

The recent GSI measurements performed using inverse kinematics for interactions of ^{208}Pb [6,7] and ^{238}U [8] at 1 GeV/nucleon and ^{197}Au at 800 MeV/nucleon [9] with liquid ^{1}H provide a very rich set of cross sections for production of practically all possible isotopes from these reactions in a "pure" form, i.e., individual cross sections from a specific given bombarding isotope (or target isotope, when considering reactions in the usual kinematics, p + A). Such cross sections are much easier to compare to models than the "camouflaged" data from γ-spectrometry measurements. These are often obtained only for a natural composition of isotopes in a target and are mainly for cumulative production, where measured cross sections contain contributions nor only from a direct production of a given isotope, but also from all its decay-chain precursors. Analysis of these new data has motivated us to further improve the CEM and to develop a preliminary version of a new code, (called CEM2k), which we describe below.

RESULTS

First, we discuss briefly the basis of the CEM and the main differences between the improved cascade-exciton model code CEM97 [3,4] and its precursor, CEM95 [2]. The CEM assumes that the reactions occur in three stages. The first stage is the IntraNuclear Cascade (INC) in which primary particles can be rescattered and produce secondary particles several times prior to absorption by, or escape from the nucleus. The excited residual nucleus remaining after the emission of the cascade particles determines the particle-hole configuration that is the starting point for the second, pre-equilibrium stage of the reaction. The subsequent relaxation of the nuclear excitation is treated in terms of the modified exciton model of pre-equilibrium decay followed by the equilibrium evaporative third stage of the reaction. Generally, all three components may contribute to experimentally measured particle spectra and distributions.

An important ingredient of the CEM is the criterion for transition from the intranuclear cascade to the pre-equilibrium model. In conventional cascade-evaporation models (like ISABEL and Bertini's INC used in LAHET [10]) fast particles are traced down to some minimal energy, the cutoff energy T_{cut} (or one compares the duration of the cascade stage of a reaction with a cutoff time, in the "timelike" INC models, like the Liege INC [11]) which is usually about 7–10 MeV above the interior nuclear potential, below which

particles are considered to be absorbed by the nucleus. The CEM uses a different criterion to decide when a primary particle is considered to have left the cascade.

An effective local optical absorptive potential $W_{opt.mod.}(r)$ is defined from the local interaction cross section of the particle, including Pauli-blocking effects. This imaginary potential is compared to one defined by a phenomenological global optical model $W_{opt.exp.}(r)$. We characterize the degree of similarity or difference of these imaginary potentials by the parameter

$$\mathcal{P} = \mid (W_{opt.mod.} - W_{opt.exp.})/W_{opt.exp.} \mid . \qquad (1)$$

When $\mathcal{P}$ increases above an empirically chosen value, the particle leaves the cascade, and is then considered to be an exciton. Both CEM95 and CEM97 use the fixed value $\mathcal{P} = 0.3$. With this value, we find the cascade stage of the CEM is generally shorter than that in other cascade models.

The transition from the preequilibrium stage of a reaction to the third (evaporation) stage occurs when the probability of nuclear transitions changing the number of excitons n with $\Delta n = +2$ becomes equal to the probability of transitions in the opposite direction, with $\Delta n = -2$, *i.e.*, when the exciton model predicts an equilibration has been established in the nucleus.

The improved cascade-exciton model as realized in the code CEM97 differs from the CEM95 version by incorporating new and better approximations for the elementary cross sections used in the cascade, using more precise values for nuclear masses, Q-values, binding and pairing energies, using corrected systematics for the level-density parameters, improving the approximation for the pion "binding energy", V_π, adjusting the cross sections of pion absorption on quasideuteron pairs inside a nucleus, considering the effects on cascade particles of refractions and reflections from the nuclear potential, allowing for nuclear transparency of pions, and including the Pauli principle in the pre-equilibrium calculation. We also make a number of refinements in the calculation of the fission channel, described separately in [4]. In addition, we have improved many algorithms used in the Monte Carlo simulations in many subroutines, decreasing the computing time by up to a factor of 6 for heavy targets, which is very important when performing practical simulations with big transport codes like MCNPX.

The authors of the GSI measurements performed a comparison of their data to several codes, including LAHET [10], YIELDX [12], ISABELA (see details and references in [8]), and the Liege INC by Cugnon [11], and encountered serious problems: none of these codes were able to accurately describe their measurements; most of the calculated distributions of isotopes produced as a function of neutron number were shifted in the direction of larger masses as compared to the data. While in some disagreement with the measurements, the Liege INC and ISABELA codes provide a better agreement with the data than LAHET and YIELDX do. Being aware of this situation with the GSI data, we decided to consider them ourselves, leading to the development of CEM2k.

First, we calculated the ^{208}Pb GSI data [6] with the standard versions of CEM95 and CEM97. As an example, Fig. 1 shows our first results obtained with the CEM95 code. Let us note that so far all CEMxx codes simulate spallation only and do not calculate any processes following fission, such as production of fission fragments and the possible evaporation of particles from them. When, during a simulation of the compound stage of a reaction these codes encounter a fission event, they simply tabulate it (allowing us to calculate the fission cross section and the fissility) and finish the calculation of this event without a subsequent calculation of fission fragments. Therefore, results from CEM95 shown in Fig. 1 reflect the contribution to the total yields of the nuclides only from deep spallation processes (successive emission of particles from the target), but do not contain fission products. This is explicitly reflected in smaller calculated cross sections for light nuclides that are produced partially or mainly by fission. We will not discuss them here. To be able to describe nuclide production in the fission region, these codes have to be extended by incorporating a model of high energy fission (*e.g.*, in the transport code MCNPX [5], where CEM97 is used, it is supplemented by the RAL fission model [13]).

One can see that though CEM95 describes quite well production of several heavy isotopes near the target (we calculate p + ^{208}Pb; therefore, for us ^{208}Pb is a target not a projectile as in the GSI measurements), it does not reproduce correctly the cross sections for lighter isotopes in the deep spallation region. The disagreement increases with increasing distance from the target, and all calculated curves are shifted to the heavy mass direction, just as was obtained by the authors of GSI measurements with all the codes they used.

The results of the CEM97 code are very similar to those of CEM95 shown in Fig. 1. Our collaborator, Dr. V. F. Batyaev of ITEP, Moscow, performed an extensive set of calculations of the same data with several more codes (HETC, LAHET with both ISABEL and Bertini options, CASCADE, CASCADE/INPE, INUCL, and YIELDX) and got very similar results [14]: all codes disagree with the data in the deep spallation region, the disagreement increases as one moves away

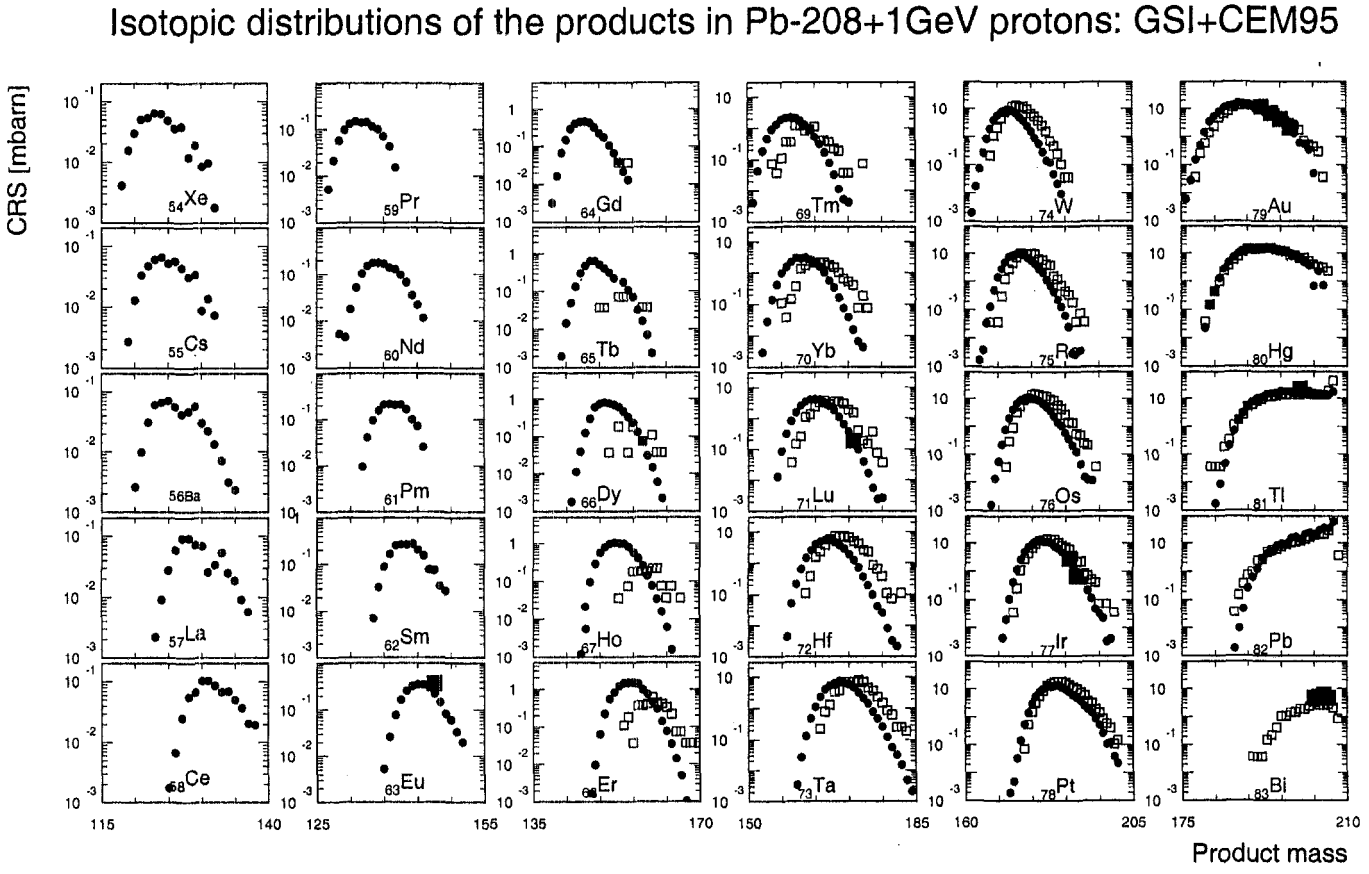

Figure 1: Comparison of isotope production cross sections from ^{208}Pb + p interaction at 1 GeV/nucleon measured at GSI [6,7] (filled circles) with the CEM95 calculations (open squares).

from the target, and all calculated curves are shifted in the heavy-mass direction.

Similar disagreements with the GSI data obtained by different authors using different codes at different laboratories suggested to us that some general features of these reactions may be treated wrong by all codes and we started to modify our CEM97 code to attempt to understand the source of the disagreement.

Fig. 2 shows some examples of steps we took in trying to determine which physical parameters might affect the discrepancies. First, according to Prokofiev's systematics [15], the value of the fission cross section for the reaction p (1 GeV) + ^{208}Pb should be $\approx$ 100 mb, i.e., only about 6% of the total reaction cross section of 1600 mb, as used by CEM97. In the past, if we were interested in describing only emitted particles and yields of the spallation products, we would not take into account fission processes in calculations of reactions with such small fission cross sections, to make the calculations faster. We would never be able predict cross sections with an accuracy better than 6%. However, since many of the isotopes are produced with quite small cross sections, there is the possibility that the variation of fission barriers with neutron and proton numbers might lead to an isotopic fractionation effect. Calculations ignoring fission are shown both in Fig. 1 for all isotopes measured at GSI [6] (CEM95) and in Fig. 2a, for production of Tl, Ir, and Tm, chosen as examples (CEM95 and CEM97). As the general agreement of calculations with the data is not good, we decided to look at the influence of fission on the production of isotopes in the spallation region. In Fig. 2b, the solid lines show calculations with CEM97 including fission, while dashed lines show the results from CEM97 (from Fig. 2a) not including fission. We see that though for most of the isotopes with high yields the two calculations almost coincide, the difference between the two calculations is somewhat larger for production of neutron-deficient isotopes of Tl (and to a lesser extent, Ir). We obtain similar results for other isotopes. This difference is large enough to lead us to the conclusion that if we hope to describe correctly production of all isotopes from a nuclear reaction, we have to take into account fission processes, even when the fission cross section itself is quite small. All the following results calculated by CEM97 are done including the fission mode, though this will not be mentioned explicitly in the text again.

We know that a currently unsolved problem of CEM97, CEM95, and, to the best of our knowledge, of most of other available codes, is the correct prediction of the complex particle yields. Usually, all codes underestimate production of ^{4}He, and to some extent, also of t and d at these incident energies. Such underestimation of complex-particle emission could affect the production of the final residual isotopes, so we decided to investigate the magnitude of this effect for our case. We are working now on better inverse cross sections used in calculating the probability for emission of complex particles and other improvements to the CEM hoping to address the problem of complex-particle yields, but for the moment we will estimate the effect of complex particle emission on residual nuclide production with a simple approximation. Our experience from analyzing other reactions involving similar energies and targets tells us that usually we underestimate the multiplicities of ^{4}He by a factor of 2, of t by a factor of 1.2, and of d by a factor of 1.1. In our model, these particles are produced only at the preequilibrium and evaporation stages of a reaction and their emission is governed by their widths. So, we multiply "by hand" the calculated widths of ^{4}He by 2, of t by 1.2, and of d by 1.1 to estimate the effect. Our results are shown in Fig. 2c) as dashed curves compared with standard CEM97 results from Fig. 2b shown as solid curves. Surprisingly, the two sets of calculations differ by little, so a simple enhancement of complex particle emission won't solve the problem of most residual nuclide yields. (Of course, for a specific isotope where α emission is an important mode of its production, the effect IS significant.)

The standard CEM97 predicts the following multiplicities for n, p, d, t, ^{3}He, and ^{4}He: 9.2409 ± 0.0025, 1.9624 ± 0.0011, 0.5518 ± 0.0006, 0.1593 ± 0.0003, 0.0682 ± 0.0002, and 0.1743 ± 0.0003, while if we enlarge the widths of ^{4}He, t, and d as described above we get, respectively, 9.0886 ± 0.0025, 1.9198 ± 0.0011, 0.5693 ± 0.0006, 0.1714 ± 0.0003, 0.0629 ± 0.0002, and 0.02743 ± 0.0004. In other words, enlarging the widths of ^{4}He, t, and d does indeed predict more ^{4}He, t, and d as it should, but at the same time fewer n and p, so that the net effect on the residual nuclides is minimal. We conclude that although the problem of complex-particle yields needs to be solved independently of the GSI data, solving this problem will not affect significantly the production of most of the final residual nuclides, so we can try to find ways of describing the GSI data without first solving the problem of complex-particle yields.

One of the things we previously noted was the fact that the calculated curves for almost all isotopes are shifted in the heavy mass direction and the shift increases as the atomic number decreases from that of the target. In other words this means that for a given final isotope (Z), all models predict emission of too few neutrons. Most of the neutrons are emitted at the evaporation stage of a reaction. So, one way to increase the

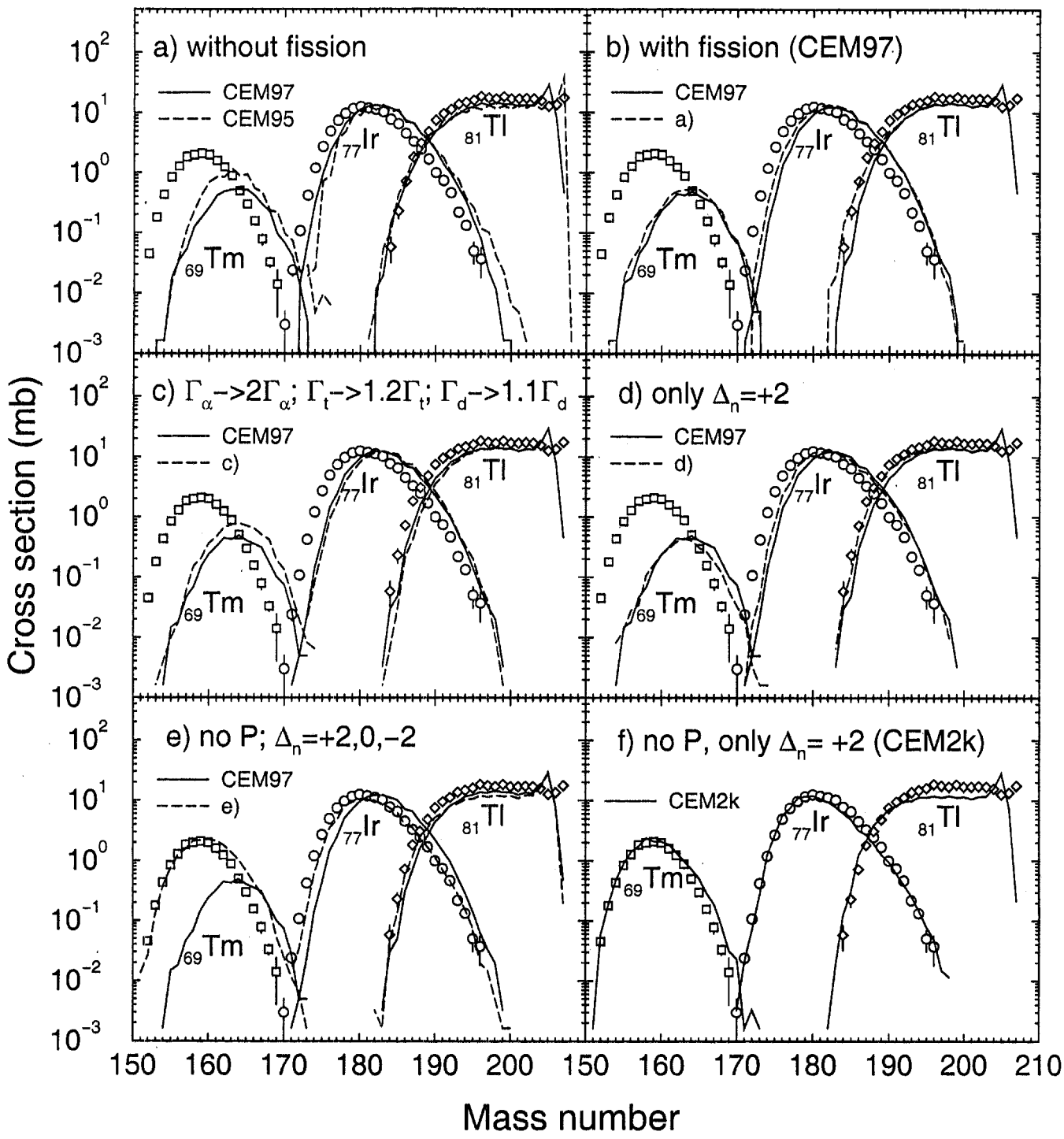

Figure 2: Example of several steps from CEM97 to CEM2k in analyzing production of ^{81}Tl, ^{77}Ir, and ^{69}Tm isotopes from ^{208}Pb interactions with ^{1}H at 1 GeV/nucleon measured at GSI [3] (see details in the text).

number of emitted neutrons would be to increase the evaporative part of a reaction. In our approach, this might be done in two different ways: the first would be to have a shorter preequilibrium stage, so that more excitation energy remains available for the following evaporation; the second would be to have a longer cascade stage of a reaction, so that after the cascade, less exciton energy is available for the preequilibrium stage, so fewer energetic preequilibrium particles are emitted, leaving more excitation energy for the evaporative stage.

Preequilibrium decay in our model involves both emission of particles from particle-like quasiparticle states, and the evolution of the number of excitons via equations for changes in exciton number of $\Delta n = +2, 0, -2$ [1]. We make the transition to evaporation when the number of excitons exceeds a critical number which depends on the nuclear mass and excitation energy. One easy way to shorten the preequilibrium stage of a reaction in CEM is to take into account only transitions that increase the number of excitons, $\Delta n = +2$, i.e., the evolution of a nucleus only torward the compound nucleus, during the equilibration. We would thus not take into account possible transitions backward, decreasing the number of excitons $\Delta n = -2$ and transitions without changing the number of excitons $\Delta n = 0$. In this case, the time of the equilibration will be shorter and fewer preequilibrium particles will be emitted, leaving more excitation energy for the evaporation. Such an approach is used by some exciton models, for instance, by the Multistage Pre-equilibrium Model used in LAHET [10]. Calculations in this modification to CEM97 are shown in Fig. 2d by dashed curves, compared with the standard CEM97 results shown by solid curves. We see that we get a slight improvement and a shift of the calculated curves in the right direction, but the effect is too small and doesn't solve the problem.

In Fig. 2e, we show the results of the second method of increasing evaporation. To enlarge the cascade part of a reaction in CEM we have either to enlarge the parameter $\mathcal{P}$ or to remove it completely and use a cutoff energy T_{cut}, as do other INC models. Our calculations have shown that a reasonable increase of $\mathcal{P}$ doesn't solve the problem. The dashed curves in Fig. 2e show calculations with CEM97 not using the parameter $\mathcal{P}$, instead using a cutoff energy of $T_{cut} = 1$ MeV, again compared with our standard CEM97 results shown by the solid curves. One can see a significant improvement of the agreement with the GSI data in this approach. Only a little more neutron emission is required to get just a perfect agreement with the data. We choose to achieve this by applying in addition to this approach the condition of taking into account only transitions with $\Delta n = +2$, discussed above in reference to Fig. 2d. Using both these conditions leads to the results shown in Fig. 2f. We call this approach CEM2k and see that it describes the GSI data very well.

The behavior of a compound nucleus in CEM is governed by its mass number, A, charge, Z, excitation energy, E^*, and its angular momentum, L (we do not have in CEM any information about the deformation of a nucleus after the preequilibrium stage of a reaction). It is informative to look at these quantities for the compound nuclei remaining after the preequilibrium stage for the different approaches discussed above. Table 1 shows values of the mean A, Z, E^* and L of the compound nuclei calculated using all the discussed approaches. One can see that as a result of the transition from CEM97 (plots a and b) to CEM2k (plot f), the mean mass and charge of the compound nuclei are almost the same, while their mean excitation energy increases by about 40 MeV. This is the main factor leading to a larger number of evaporated neutrons, and as a consequence, to a much better agreement with the GSI data.

Table 1: Mean mass number A, charge Z, excitation energy E^* (MeV), and angular momentum L ($\hbar$) of the compound nuclei formed after the preequilibrium stage of reactions calculated by the different approaches as plotted in Fig. 2

Method	A	Z	E^*	L
CEM97 (plots a and b)	193.9	78.2	58.7	24.6
$\Gamma_\alpha \to 2\Gamma_\alpha$ (plot c)	193.4	78.0	58.3	24.8
Only $\Delta_n = +2$ (plot d)	196.4	78.6	86.4	24.1
No $\mathcal{P}$ (plot e)	191.0	77.5	65.0	21.3
CEM2k (plot f)	193.9	78.1	97.5	20.8

In short, CEM2k has a longer cascade stage, less preequilibrium emission, and a longer evaporation stage with a higher excitation energy, as compared to CEM97 and CEM95.

Fig. 3 shows a comparison of the CEM2k results with all the data (excluding those involving fission-fragment production) on isotope yields measured at GSI for the reaction ^{208}Pb + p. There is a very good agreement for almost all isotopes.

A comparison of the CEM2k results with predictions by CEM95 [2], LAHET-ISABEL [10], LAHET-Bertini [10], CASCADE/INPE [17], CASCADE [18], YIELDX

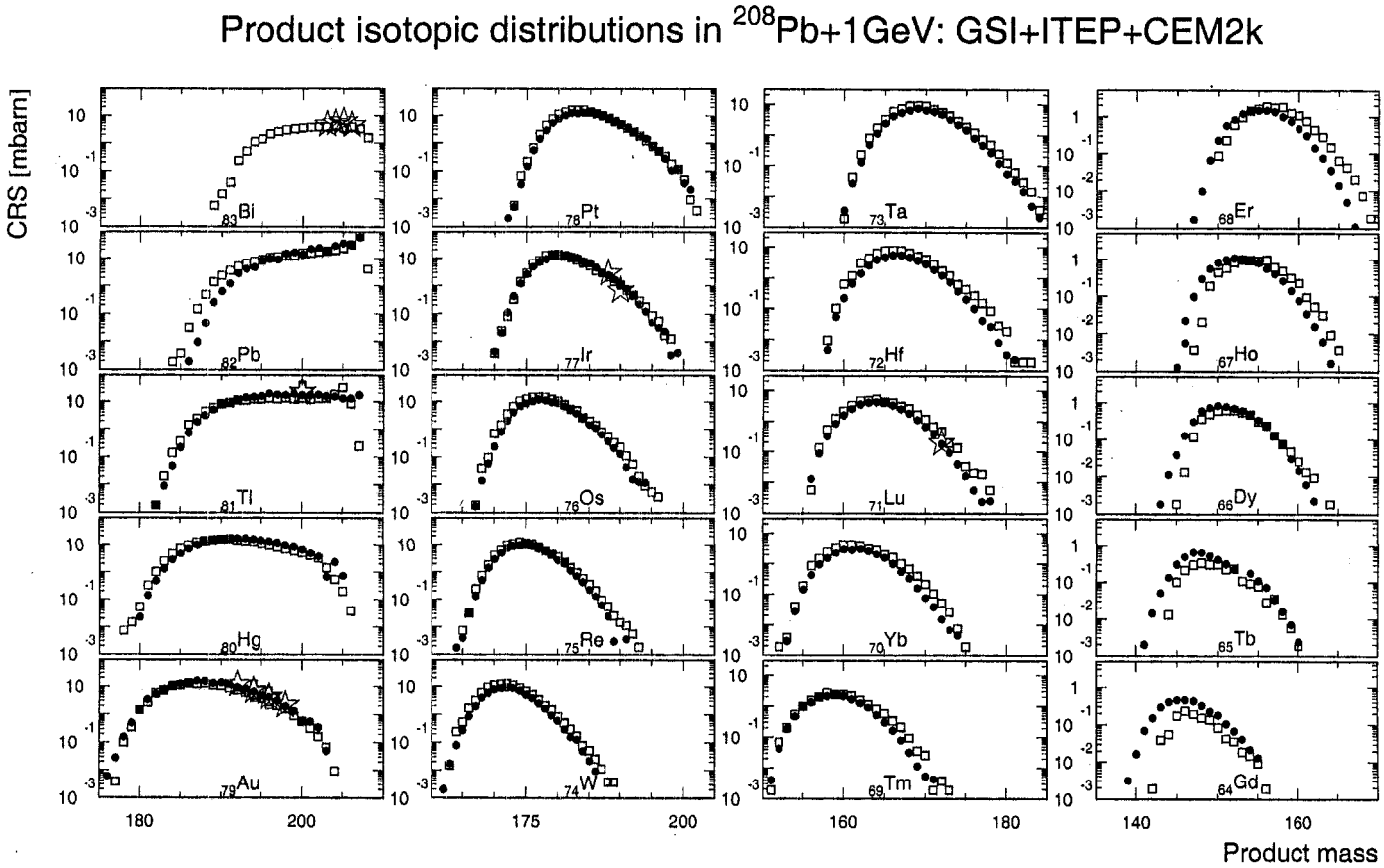

Figure 3: Isotopic production cross sections of elements between Z=64 and 83 in the reaction of ^{208}Pb on hydrogen at 1 GeV/nucleon. Filled circles show GSI data [6], open stars are recent ITEP data measured by the γ-spectrometry method [16], while open squares show our CEM2k results.

[12], and INUCL [19] codes together with the GSI [6] and ITEP [16] data from our recent paper [16] is shown in Fig. 4. One can see that CEM2k agrees best with the data of the other codes tested here.

Finding a good agreement of CEM2k with the isotope production yields, we wish to see how well it describes spectra of secondary particles in comparison with its precursor, CEM97. Fig. 4 shows examples of neutron spectra from interactions of protons with the same target, ^{208}Pb at 0.8 Gev and 1.5 GeV (we do not know of measurements of spectra at 1 GeV, the energy of isotope-production yield data). We see that CEM2k describes spectra of secondary neutrons certainly no worse than does CEM97, but possibly a little better at larger angles, in a good agreement with the data. So this preliminary version of an improved CEM code, CEM2k, describes both the GSI data from ^{208}Pb interactions with p at 1 GeV/nucleon and the spectra of emitted neutrons from p+^{208}Pb at 0.8 and 1.5 GeV better than its precursor CEM97.

Besides the ^{208}Pb data discussed above, reactions induced by ^{197}Au at 800 MeV/nucleon [9] and ^{238}U at 1 GeV/nucleon [8] were measured recently at GSI. We use CEM2k as fixed from our analysis of the ^{208}Pb data [6,7] without further modifications to calculate the ^{197}Au measurements [9]. Our CEM2k results are shown in Figs. 6 and 7 together with standard CEM97 predictions and calculations by LAHET-Bertini [10] and YIELDX [12] codes from [9]. We see that just as in the case of the ^{208}Pb data, CEM2k agrees best with the ^{197}Au data in the spallation region compared to the other codes tested here. For the production of nuclides lighter than Tb (Fig. 7), where fission-fragment formation begins to contribute, CEM2k underestimates the data (it doesn't include a model of fission-fragment production, as we discussed previously).

The ^{238}U GSI data are still preliminary (with relative errors of 40%), published only as figures [8] and not available yet in tabulated form. These data are of a great interest to us as the reaction mechanisms in the case of p + ^{238}U interactions differ significantly from those of ^{208}Pb and ^{197}Au targets. Again, according to Prokofiev's systematics [15], for the reaction p (1 GeV) + ^{238}U the fission cross section is about 1390 mb, which makes up about 80% of the total reaction

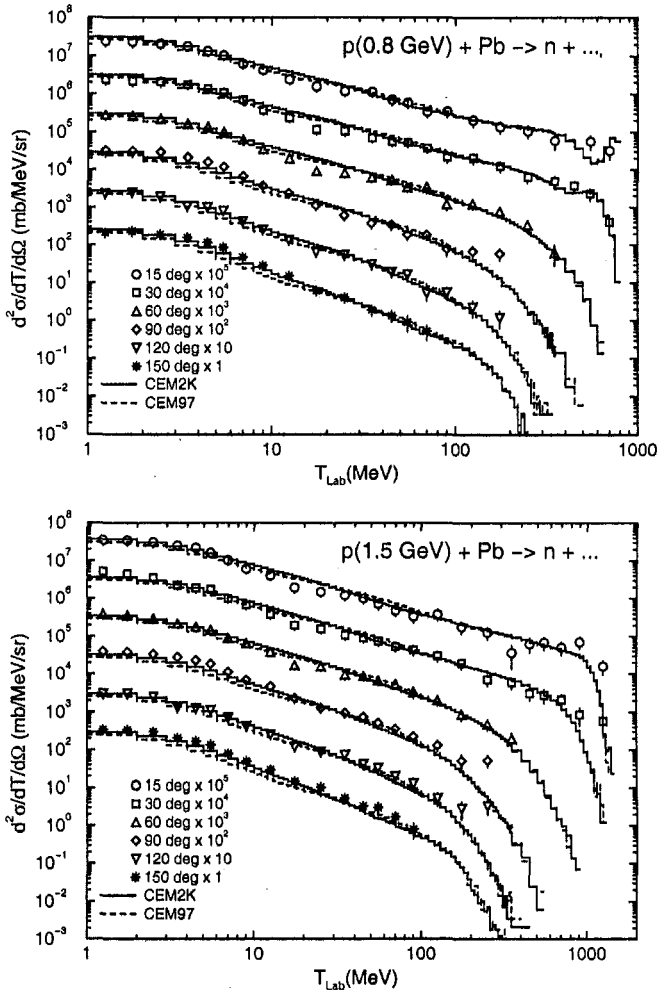

Figure 5: Comparison of measured [20] double differential cross sections of neutrons from 0.8 and 1.5 GeV protons on Pb with CEM2k and CEM97 calculations.

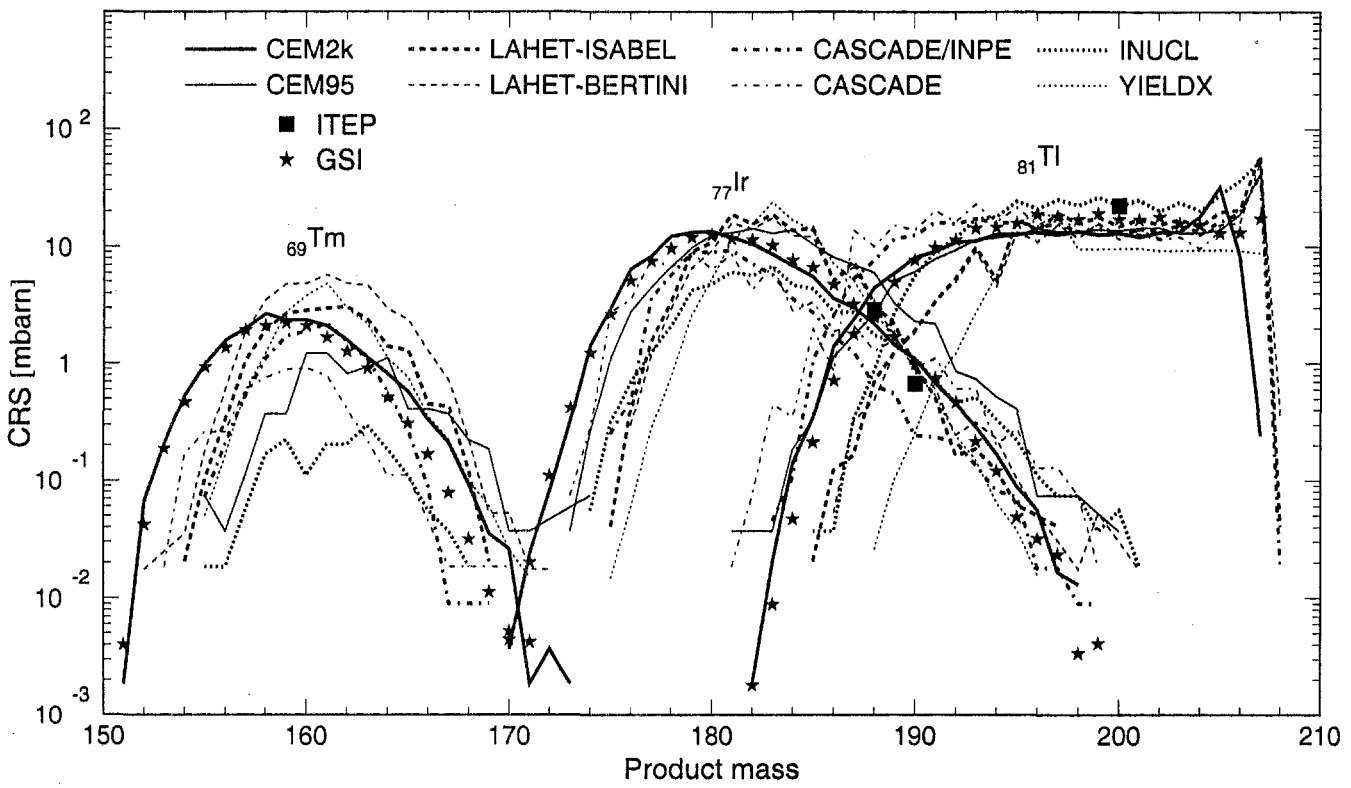

Figure 4: Isotopic mass distributions for independent production of Tm, Ir, and Tl isotopes from 1 GeV protons colliding with ^{208}Pb. Squares are ITEP measurements [16], while stars show GSI data obtained in reverse kinematics [6]. Results from different codes are marked as: CEM2k—our results, CEM95—Ref. [2], LAHET-ISABEL—Ref. [10], LAHET-Bertini—Ref. [10], CASCADE/INPE—Ref. [17], CASCADE—Ref. [18], INUCL—Ref. [19], and YIELDX—Ref. [12].

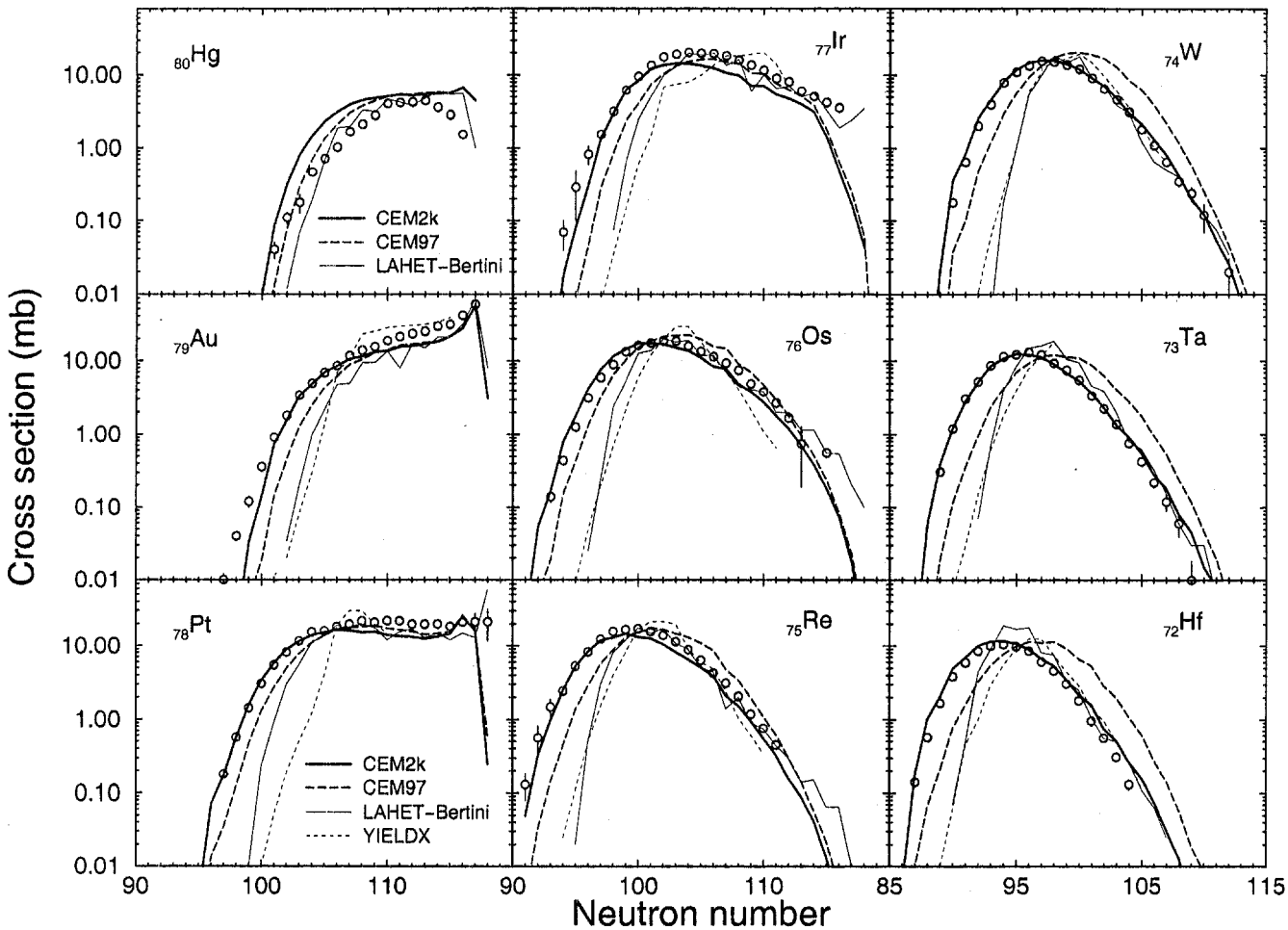

Figure 6: Isotopic distribution of the spallation products from the reaction ^{197}Au + p at 800 A MeV from mercury to hafnium. Open circles are the GSI data [9], CEM2k (thick solid curves) and CEM97 (thick dashed curves) are our present calculations, LAHET-Bertini (thin solid curves) and YIELDX (thin dashed curves) are results of calculations from [9].

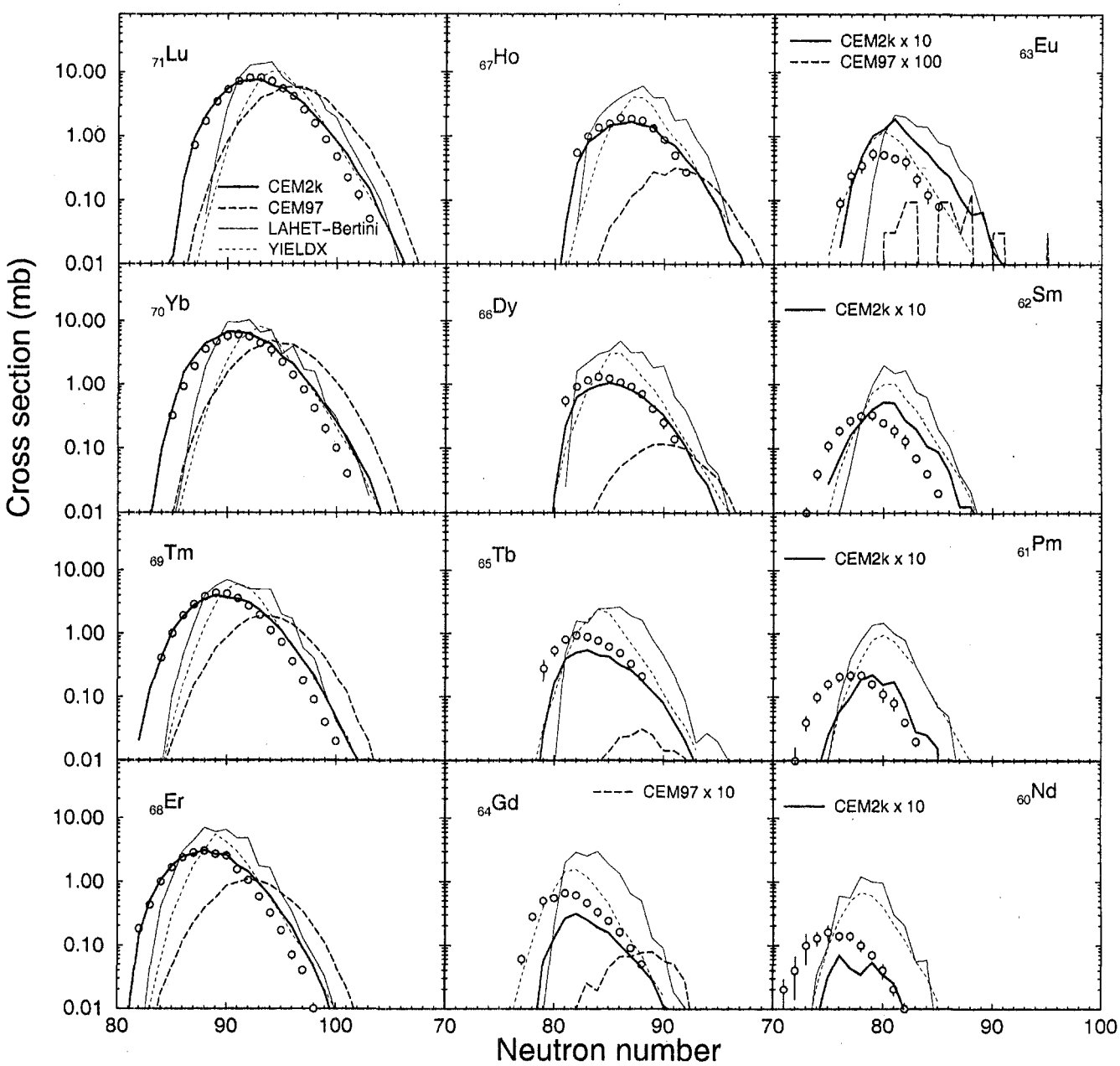

Figure 7: The same as Fig. 6 but for products from lutetium to neodymium.

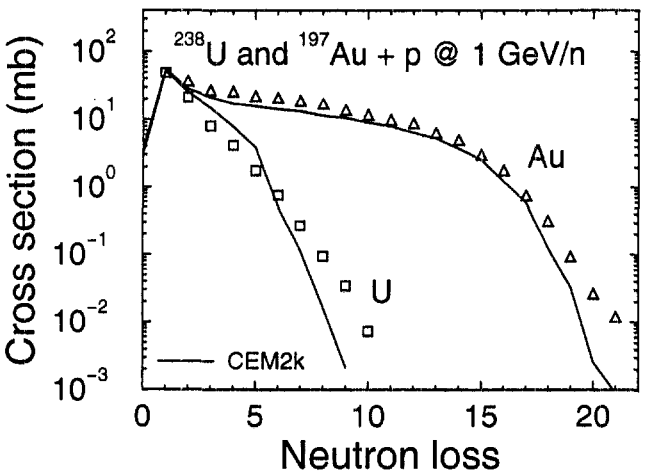

Figure 8: Comparison of the production of projectile isotopes in gold and uranium interactions with liquid hydrogen targets as measured at GSI [8] (symbols) and predicted by CEM2k (curves).

cross section of 1788 mb as calculated by CEM2k. This means that fission is the main mode for this reaction and almost everything in a model prediction of isotope production should be determined by how well the model describes the neutron-to-fission width ratio, Γ_n/Γ_f. So, the ^{238}U GSI data will be very useful to test and improve the treatment of the fission mode by any code, including CEM2k. We enlarged the figures from [8], to get (approximate!) numerical values of measured cross sections, and calculated this reaction with CEM2k.

As an example, Fig. 8 shows the a comparison of our CEM2k calculations with the GSI data [8] on production of uranium isotopes from p (1 GeV) interactions with ^{238}U and of gold isotopes from proton interactions with ^{197}Au. The agreement of CEM2k with ^{238}U data is not as good as for ^{197}Au, or as observed above for ^{208}Pb at 1 GeV/nucleon and ^{197}Au at 800 MeV/n. This means we still have room for CEM2k improvement, especially in the treatment of the fission mode. At the same time, Fig. 8 demonstrates how different are the reaction mechanisms in ^{197}Au and ^{238}U: while 21 isotopes of gold were measured from ^{197}Au, only 10 isotopes of uranium were measured from ^{238}U, and their yield decreases exponentially as one moves into the neutron-deficient region, a direct result of the dominant role of the fission mode in uranium.

FURTHER WORK

Besides the changes to CEM97 mentioned above, we also made a number of other improvements and refinements, such as imposing momentum-energy conservation for each simulated event (the Monte Carlo algorithm previously used in CEM provides momentum energy conservation only statisticaly, on average, but not exactly for each simulated event); using real binding energies for nucleons at the cascade stage of a reaction instead of the approximation of a constant separation energy of 7 MeV used in previous versions of the CEM; using reduced masses of particles in the calculation their emission widths instead of using the approximation of no-recoil used in previous versions; coalescence of complex particles from fast cascade nucleons already outside the nucleus. These refinements are important physically, and they slightly improve the agreement of calculations with the data, but not so dramatically as the changes discussed above. For this reason we do not show here figures with examples. In addition, CEM2k is still under development and will still change. We need to analyze a lot of more available data with it, especially at lower incident energies. We plan also to incorporate better inverse cross sections and to solve a problem of overestimation of fission cross sections at energies above 1 GeV, observed recently in our preliminary calculations of the p (2.6 GeV) + Hg reaction [21]. When we complete CEM2k to a reasonable level, we plan to incorporate it into LAHET and to replace the present CEM97 in MCNPX.

ACKNOWLEDGMENTS

We thank Dr. B. Mustapha for sending us tables with GSI data for ^{208}Pb and ^{197}Au and express our gratitude to Drs. S. Chiba and K. Ishibashi for suppling us with numerical values of their neutron spectra measurements. We are grateful to Drs. L. S. Waters and R. E. Prael for useful discussions, interest, and support.

This study was supported by the U. S. Department of Energy.

REFERENCES

1. K. K. Gudima, S. G. Mashnik, and V. D. Toneev, "Cascade-Exciton Model of Nuclear Reactions," *Nucl. Phys.* **A401**, 329 (1983).
2. S. G. Mashnik, "User Manual for the Code CEM95," JINR, Dubna (1995); OECD NEA Data Bank, Paris, France (1995); http://www.nea.fr/abs/html/iaea1247.html; RSIC-PSR-357, Oak Ridge, 1995.
3. S. G. Mashnik and A. J. Sierk, "Improved Cascade-Exciton Model of Nuclear Reactions," *Proc. Fourth Workshop on Simulating Accelerator Radiation Environments (SARE4)*, Knoxville, TN, USA, September 14–16, 1998, T. A. Gabriel, Ed., ORNL (1999) pp. 29–51.

4. A. J. Sierk and S. G. Mashnik, "Modeling Fission in the Cascade-Exciton Model," *Proc. Fourth Workshop on Simulating Accelerator Radiation Environments (SARE4)*, Knoxville, TN, USA, September 14–16, 1998, T. A. Gabriel, Ed., ORNL (1999) pp. 53–67.

5. *MCNPX^{TM} User's Manual, Version 2.1.5*, edited by Laurie S. Waters, Los Alamos National Laboratory Report LA-UR-99-6058 (1999).

6. W. Wlazlo, T. Enqvist, P. Armbruster, J. Benlliure, M. Bernas, A. Boudard, S. Czájkowski, R. Legrain, S. Leray, B. Mustapha, M. Pravikoff, F. Rejmund, K.-H. Schmidt, C. Stéphan, J. Taieb, L. Tassan-Got, and C. Volant, "Cross Sections of Spallation Residues Produced in 1*A* GeV ^{208}Pb on Proton Reactions," *Phys. Rev. Lett.* **84**, 5736 (2000).

7. T. Enqvist, W. Wlazlo, P. Armbruster, J. Benlliure, M. Bernas, A. Boudard, S. Czájkowski, R. Legrain, S. Leray, B. Mustapha, M. Pravikoff, F. Rejmund, K.-H. Schmidt, C. Stéphan, J. Taieb, L. Tassan-Got, and C. Volant, "Isotopic Yields and Kinematic Energies of Primary Residues in 1*A* GeV ^{208}Pb + p Reactions," GSI Preprint 2000-28, http://www-wnt.gsi.de/kschmidt/publica.htm, submitted to *Nucl. Phys. A*.

8. J. Taieb, P. Armbruster, J. Benlliure, M. Bernas, A. Boudard, S. Czájkowski, T. Enqvist, F. Rejmund, R. Legrain, S. Leray, B. Mustapha, M. Pravikoff, K.-H. Schmidt, C. Stéphan, L. Tassan-Got, C. Volant, and W. Wlazlo, "Measurement of ^{238}U Spallation Product Cross Sections at 1 GeV per Nucleon," http://www-wnt.gsi.de/kschmidt/publica.htm#Conferences.

9. F. Rejmund, B. Mustapha, P. Armbruster, J. Benlliure, M. Bernas, A. Boudard, J. P. Dufour, T. Enqvist, R. Legrain, S. Leray, K.-H. Schmidt, C. Stéphan, J. Taieb, L. Tassan-Got, and C. Volant, "Measurement of Isotopic Cross Sections of Spallation Residues in 800 *A* MeV ^{197}Au + p Collisions," GSI Preprint 2000-06, http://www-wnt.gsi.de/kschmidt/publica.htm, submitted to *Nucl. Phys. A*.

10. R. E. Prael and H. Lichtenstein, "User guide to LCS: The LAHET Code System," LANL Report No. LA-UR-89-3014, Los Alamos (1989); http://www-xdiv.lanl.gov/XTM/lcs/lahet-doc.html.

11. J. Cugnon, C. Volant, and S. Vuillier, "Improved Intranuclear Cascade Model for Nucleon-Nucleus Interactions, *Nucl. Phys.* **A620**, 475 (1997).

12. R. Silberberg, C. H. Tsao, and A. F. Barghouty, "Updated Partial Cross Sections of Proton-Nucleus Reactions," *Astrophys. J.* **501**, 911 (1998); R. Silberberg and C. H. Tsao, "Partial Cross-Sections in High-Energy Nuclear Reactions, and Astrophysical Applications. I. Targets With $Z \leq 28$," *Astrophys. J. Suppl.*, No. 220, **25**, 315 (1973); R. Silberberg and C. H. Tsao, "Partial Cross-Sections in High-Energy Nuclear Reactions, and Astrophysical Applications. II. Targets Heavier Than Nickel," *ibid*, p. 335.

13. F. Atchison, "Spallation and Fission in Heavy Metal Nuclei under Medium Energy Proton Bombardment," in *Targets for Neutron Beam Spallation Source*, Jul-Conf-34, Kernforschungsanlage Julich GmbH (January 1980).

14. V. F. Batyaev, private communication, June 2000, and to be published.

15. A. V. Prokofiev, "Compilation and Systematics of Proton-Induced Fission Cross Section Data," *Nucl. Instrum. Meth. A*, to be published in 2000.

16. Yu. E. Titarenko, O. V. Shvedov, V. F. Batyaev, E. I. Karpikhin, V. M. Zhivun, A. B. Koldobsky, R. D. Mulambetov, D. V. Fischenko, S. V. Kvasova, A. N. Sosnin, S. G. Mashnik, R. E. Prael, A. J. Sierk, T. A. Gabriel, M. Saito, and H. Yasuda, "Cross Sections for Nuclide Production in 1 GeV Proton-Irradiated ^{208}Pb," LANL Report LA-UR-00-4779, Los Alamos (2000), submitted to Phys. Rev. C.

17. V. S. Barashenkov, A. Yu. Konobeev, Yu. A. Korovin, and V. N. Sosnin, "CASCADE/INPE Code System," *Atomic Energy*, **87**, 742 (1999).

18. V. S. Barashenkov, Le Van Ngok, L. G. Levchuk, Zh. Zh. Musul'manbekov, A. N. Sosnin, V. D. Toneev, and S. Yu. Shmakov, JINR Report R2-85-173, Dubna, 1985; V. S. Barashenkov, F. G. Zheregi, and Zh. Zh. Musul'manbekov, *Sov. J. Nucl. Phys.*, **39**, 715 (1984); V. S. Barashenkov, B. F. Kostenko, and A. M. Zadorogny, *Nucl. Phys.*, **A338**, 413 (1980).

19. G. A. Lobov, N. V. Stepanov, A. A. Sibirtsev, and Yu. V. Trebukhovskii, Institute for Theoretical and Experimental Physics (ITEP) Preprint No. ITEP-91, Moscow, 1983; A. A. Sibirtsev, N. V. Stepanov, and Yu. V. Trebukhovskii, ITEP Preprint No. ITEP-129, Moscow, 1985; N. V. Stepanov, ITEP Preprint No. ITEP-81, Moscow, 1987; N. V. Stepanov, ITEP Preprint No. ITEP-55-88, Moscow, 1988 (in Russian).

20. K. Ishibashi, H. Takada, T. Nakomoto, N. Shigyo, K. Maehata, N. Matsufuji, S. Meigo, S. Chiba, M. Numajiri, Y. Watanabe, T. Nakamura,

"Measurement of Neutron-Production Double-Differential Cross Sections for Nuclear Spallation Reaction Induced by 0.8, 1.5 and 3.0 GeV Protons," *J. Nucl. Sci. Techn.*, **34**, 529 (1997).

21. Yu. E. Titarenko, O. V. Shvedov, V. F. Batyaev, V. M. Zhivun, E. I. Karpikhin, R. D. Mulambetov, D. V. Fischenko, S. V. Kvasova, , S. G. Mashnik, R. E. Prael, A. J. Sierk, and H. Yasuda, "Study of Residual Product Nuclide Yields From 0.1, 0.2, 0.8, and 2.6 GeV Proton-Irradiated ^{nat}Hg Targets," LANL Report LA-UR-00-3600, Los Alamos (2000); E-print nucl-ex/0008012 21 Aug 2000; to be published in *Proceedings of the Fifth International Workshop on Shielding Aspects of Accelerators, Irradiation and Target Facilities (SATIF5)*, July 18–21, 2000, OECD Headquarters, Paris, France.